STScI | SPACE TELESCOPE SCIENCE INSTITUTE

Instrument Science Report COS 2021-02(v1)

Cycle 27 COS/FUV Spectroscopic Sensitivity Monitor

Ravi Sankrit[1] & Kate Rowlands[1]

[1] Space Telescope Science Institute, Baltimore, MD

8 March 2021

ABSTRACT

The Cycle 27 COS/FUV spectroscopic sensitivity monitor ran from December 2019 to October 2020. The standard modes and the new modes (G160M/1533 and G140L/800, introduced in Cycle 26) observations were obtained at Lifetime Position 4 (LP4), the nominal position for COS starting October 2, 2017, and the blue modes (G130M/1055 and G130M/1096) were obtained at Lifetime Position 2 (LP2). The Time-Dependent Sensitivity (TDS) slopes of all modes were found to remain within the range 0% to −4% per year. However, the standard mode slopes were systematically diverging from the existing TDS model. A new hybrid cenwave dependent model was introduced, where for monitored cenwaves, the slopes are determined only from observations obtained using that cenwave, while for unmonitored cenwaves, the slopes continue to be averaged as before. The TDSTAB reference file was updated with new parameters for the standard modes to correct for these divergences. In this ISR we describe the program and its execution, provide a summary of the analysis and results, and motivate and describe the newly introduced hybrid cenwave dependent derivation of the TDS parameters.

Contents

1. Introduction

The initial discovery of declines in sensitivity in several COS spectroscopic modes was reported by Osten et al. (2010). Monitoring programs were initiated to follow these trends. The Far-Ultraviolet (FUV) Time-Dependent Sensitivity (TDS) monitoring programs, and their results have been described in a series of publications (Osten et al. 2011, Bostroem et al. 2014, De Rosa et al. 2016, 2017, 2018, Sankrit 2019, 2020). The temporal sensitivity variations are modeled as functions of wavelength for each combination of grating (G130M, G160M, G140L) and segment (FUVA, FUVB). These are included in the TDS reference file, TDSTAB, which is used in CalCOS in association with the photometric throughput reference file, FLUXTAB, to obtain flux calibrated data.

The Cycle 27 FUV TDS monitor (PID: 15773, PI: R. Sankrit) consisted of observations of the flux calibration standards, GD71 and WD0308-565, with the plan of obtaining data every two months between December 2019 and October 2020.

2. Program Design

The FUV TDS program is designed to obtain regular observations of flux calibration standards using the shortest and longest central wavelength standard settings of each grating, and additionally G130M/1222 (first offered to the community in Cycle 20), and the "blue modes", G130M/1055 and G130M/1096. Two modes, the "new cenwaves", G160M/1533 and G140L/800 were introduced at the beginning of Cycle 26 and were added to the regularly monitored modes starting with the second set of visits in the Cycle 26 monitoring program (Sankrit 2020).

The two white dwarf standards, GD71 and WD0308-565, have been used for the FUV TDS monitor since the move to LP2 in Cycle 20. The choice of target for each cenwave and segment is based on optimizing the signal-to-noise ratio (S/N) achieved, while minimizing the impact on detector lifetime.

The exposure times were determined by requiring a S/N of 15 per resel at the wavelength of least sensitivity for each of the standard modes, except G130M/1222, and for the new cenwave G140L/800. For the blue modes and for G130M/1222, the

Table 1. Modes Tracked using GD71

Grating	Cenwave	Segment	t_{exp} (sec)
G130M	1096	B	744
G160M	1533	A	103
	1577	A	132
	1623	A	172

Table 2. Modes Tracked using WD0308-565

Grating	Cenwave	Segment	t_{exp} (sec)
G130M	1055	A	363
	1222	both	254
	1291	both	233
	1327	A	278
G160M	1533	B	222
	1577	B	273
	1623	B	369
G140L	800	A	363
	1105	A	327
	1280	both	328

goal was to obtain S/N$\sim$25 per resel at the wavelength of maximum sensitivity, which ensured that S/N$>$15 for $\lambda > 1030$ Å for G130M/1096/FUVB, and for $\lambda > 1130$ Å for G130M/1055/FUVA and G130M/1222. For G140L/800, the goal was to obtain S/N of 15 per resel at the wavelength of least sensitivity longward of 1150 Å. Below this threshold the throughput is low because of the sharp drop in reflectivity of the HST MgF_2/Al primary mirror. The exposure time used for this setting provides S/N of between 30 and 40 per 20Å bin at these wavelengths.

The resulting total exposure times, plus overheads require two orbits per visit for GD71 and three orbits per visit for WD0308-565. GD71 is too bright to observe using G130M/1096/FUVA, and there are no lamp lines available in the wavelength range covered by 1096/FUVB, therefore the GD71 visitis include a wavelength calibration lamp observation through 1096/FUVA that is obtained immediately after the science exposure, at the same Optics Select Mechanism 1 (OSM1) position.

The modes tracked in the Cycle 27 program with GD71 and WD0308-565, and the exposure times used are listed in Tables 1 and 2, respectively. The exposure times

are the same as those used in Cycle 26. The mode G130M/1327/FUVB, which was monitored up until Cycle 24 is not observed any longer as a consequence of the COS 2025 policy (Oliveira et al. 2018).

The visit structure and sequence of observations in the Cycle 27 program follows the "complete monitoring sequence" implemented in Cycle 24 (PID: 14854, PI: G. De Rosa), described in De Rosa (2018), with the addition of the new cenwaves starting in February 2019 (Cycle 26). The analyses of the Cycle 24 data showed that the "reduced monitoring sequence" observations (consisting of only G130M/1291, G160M/1623, and G140L/1280, and executed every alternate month) were not necessary, and therefore were dropped starting in the Cycle 25 program.

The standard mode and new cenwave observations were obtained at the nominal (current) COS FUV lifetime position (LP4), while the blue modes are observed at LP2. In all cases, the observations were obtained at FP-POS 3 only.

3. Observations

The data used in the regular FUV TDS analysis were based on the set of observations shown in Table 3, organized by the observation date. The original program included six visits for WD0308-565, and five for GD71, which is not visible between the end of April and the beginning of August. The program was impacted by two failed visits, 03 and 04, and the observations were repeated in visits 53 and 54, respectively. Visits 07 and 08 were only partly successful, and the failed observations were repeated in visits 57 and 58, respectively. All the data from successful observations are available in the archive.

4. Analysis and Results

4.1 Regular TDS Monitor

The data were analyzed following the method described in Bostroem (2014), and using the script, *cos_tds_analysis.py*. Calibrated `_x1d.fits` files obtained as part of the FUV TDS monitoring programs from 2009 through October 2020 were used in the analysis. The net counts were binned over 5 Å for the medium resolution modes, and over 20 Å for the low resolution modes. The data obtained at LP2, LP3, and LP4, are scaled to data obtained at LP1, LP2 and LP3, respectively using contemporaneous observations obtained at the different LPs. Preliminary fits to the data using a piecewise-linear function with breakpoints at decimal years 2010.20, 2011.20, 2011.75, 2012.00, 2012.80, 2013.80, and 2015.50 indicated the need for a new breakpoint. After some experimentation, a new breakpoint at 2019.0 was introduced and the fits to data were obtained. The overall relative sensitivity was normalized to 1.0 at the time of first light (May 01, 2009). Fig. 1 shows a summary plot of the sensitivity against time. Also plotted for comparison is the solar activity directed towards the

Table 3. Regular Program Observation Dates

Obs. Date	Visit No.	Target
2019-Dec-30	02	GD71
2019-Dec-31	01	WD0308-565
2020-Mar-11	54	GD71
2020-Mar-16	53	WD0308-565
2020-Apr-10	06	GD71
2020-Apr-16	05	WD0308-565
2020-Jun-17	07[a]	WD0308-565
2020-Jul-12	57	WD0308-565
2020-Aug-09	08[b]	WD0308-565
2020-Aug-16	09	GD71
2020-Aug-31	58	WD0308-565
2020-Oct-06	10	WD0308-565
2020-Oct-17	11	GD71

[a]Partial failure; c800, 1105, 1327 repeated in visit 57.

[b]Partial failure, c1533, 1577, 1623, 800, 1105, 1327 repeated in visit 58.

earth as a function of time. The 10.7 cm solar fluxes are obtained periodically from the Solar Monitoring Program hosted by Natural Resources Canada at https://www.spaceweather.gc.ca/solarflux/sx-en.php .

The TDS slopes for the linear fits between 2015.5 and 2019.0, and since 2019.0 are relatively uniform over the COS wavelength range, varying between approximately 0% and -4% per year. In Fig. 2 the TDS slopes are shown plotted against wavelength for each grating and segment for these two time intervals.

Systematic divergences of the measured TDS slopes compared with the models were noticed at the edges of the FUVA detector during Cycle 26 (Sankrit 2020). The slopes were steeper than the models at the short-wavelength end, and shallower at the long wavelength end. These divergences caused the absolute and relative flux accuracies of the standard modes to exceed their requirements of 5% and 2%, respectively (Fig. 3). Furthermore, it became evident during Cycle 27 that for the FUVB detector the TDS slope was steeper than the model over the entire wavelength ranges and also approaching the tolerance limits.

The update to the standard modes TDSTAB reference tables, which was planned when the divergences were first noticed has now been completed, and a new TDSTAB file was delivered. In a parallel effort, the flux calibration of the blue-modes was redone, and led to the creation of a new set of calibration parameters including the sensitivities used in the FLUXTAB and the slopes used in the TDSTAB reference files. These are

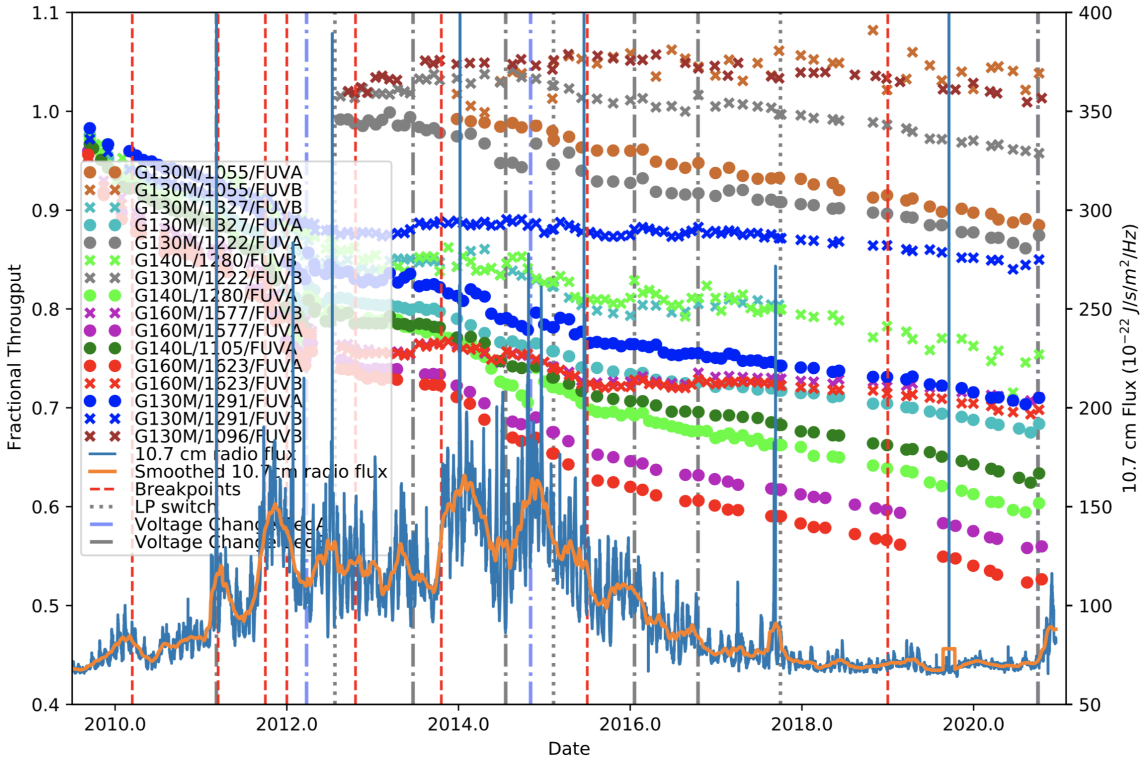

Figure 1. The change in COS FUV spectroscopic sensitivity with time. The fractional throughput, relative to first light, is shown for each mode tracked as a function of decimal year. The solar activity directed at Earth, as measured by the 10.7 cm flux is shown as a solid blue line (overlaid with a smoothed version in orange). Dashed red vertical lines show the breakpoints used in the piecewise linear function that models the TDS. The dates of the LP moves are shown as dotted grey lines, and the dot-dashed lines indicate when the operational voltage was changed.

described in forthcoming ISRs, Dieterich et al. (2021) and Rowlands et al. (2021).

The standard modes TDS parameters were derived partially accounting for the cenwave dependence of the slopes. The necessity for this modified procedure, and an outline of the steps are described in the next section.

4.2 Hybrid Cenwave Dependent TDSTAB

The TDS is modeled as a piece-wise linear function of time for each grating and detector segment combination, dependent on, and smoothly varying with wavelength. As described in the ISR, the sensitivity is monitored using a subset of the available cenwaves for each grating, which cover the full band-pass. The slopes of sensitivity against time are determined for each monitored cenwave. Until now, the TDS reference file used slopes that were averaged at each wavelength bin and then smoothed over

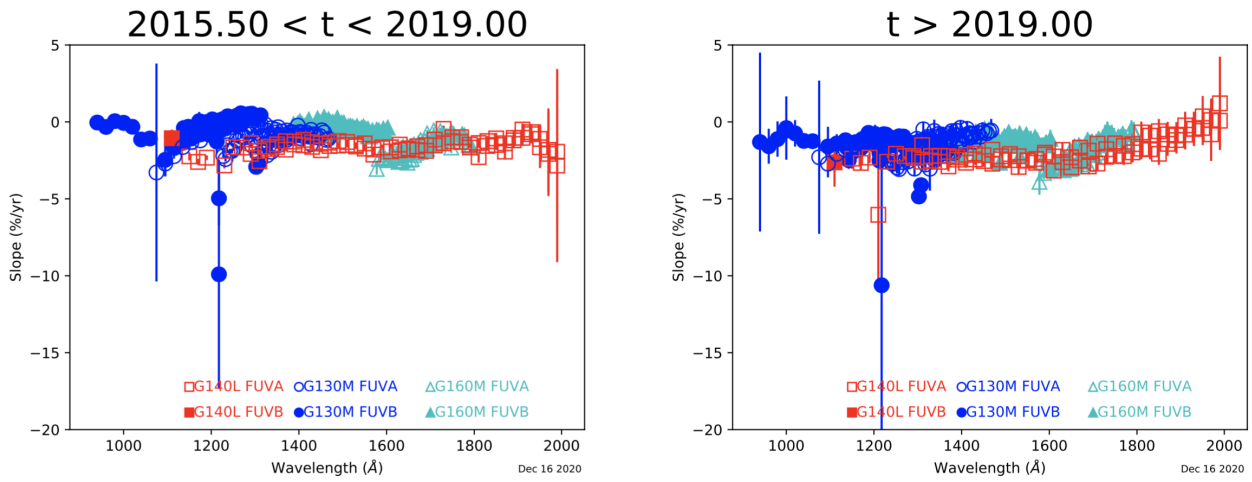

Figure 2. The COS TDS slopes obtained at the end of the regular Cycle 27 observations (October 2020) expressed in percentage change per year plotted against wavelength for the different gratings and segments. The left panel shows the slopes between 2015.5 and 2019.0, the newly introduced breakpoint, and right panel shows the slope since 2019.0. Note that the G140L, FUVB slope is a for a single 20 Å bin in the cenwave 1280 setting. The errors on the derived slopes are small except in some cases near the detector edges, and around airglow lines.

several wavelength bins. These slopes were used for all cenwaves, including those being monitored. This method does not allow for sensitivity variations that are not dependent on wavelength, but instead on the detector location.

Monitoring data over the last few cycles showed evidence for sensitivity changes that were detector location dependent. Anticipating that these dependencies would need to be accounted for in the TDS modeling, the format of the TDSTAB reference file was changed to make the parameters cenwave dependent rather than grating dependent (Interface Control Document ICD-47, section 12.3.1). When the new format TDSTAB was first implemented, the parameters were copied over from the old format reference file. We have used a modified approach to derive the new TDS paramaters: for each monitored cenwave, only data obtained using that cenwave were used in deriving the slopes, while for the unmonitored cenwaves, the averaging was done exactly as before.

To illustrate the need and impact of this change, we consider the specific example of the G160M grating, segment FUVA, which is monitored using observations of GD71. The cenwaves used for the standard modes TDS are G160M/1577 for which segment A spans 1578–1749 Å and G160M/1623, for which the coverage is 1625–1796 Å. Fig. 4 shows the derived slopes for these two cenwaves in the last time-bin (i.e. observation dates later than 2019.0). The cenwave 1577 slopes are in purple, and the cenwave 1623 slopes in red. The yellow line shows the average slope for each wavelength bin (5 Å for these modes) smoothed by 11 bins. Since the 2019.0 breakpoint has been newly

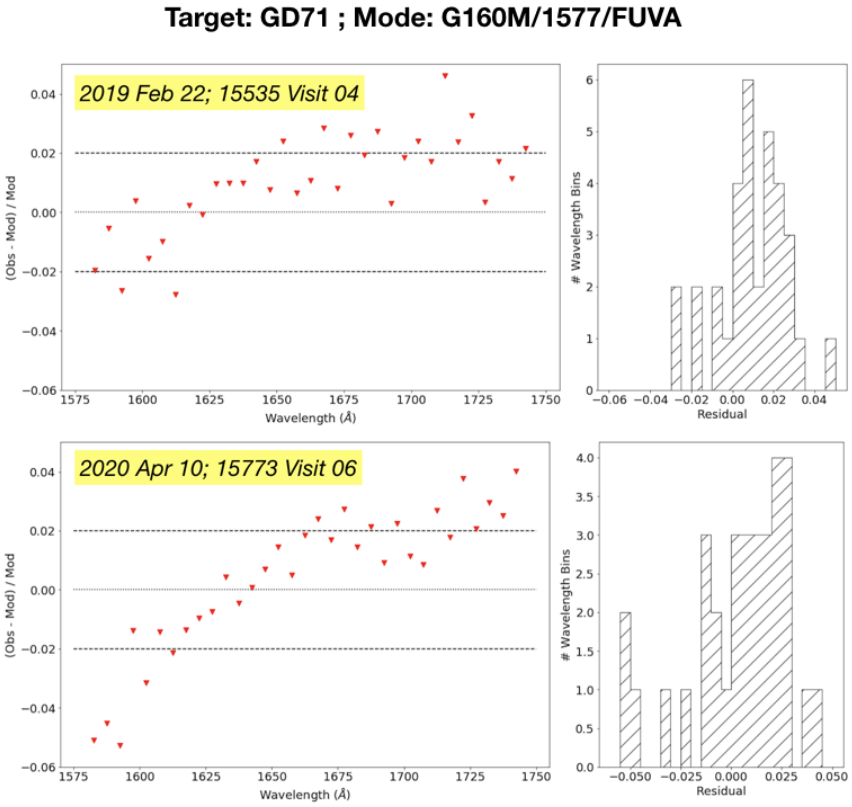

Figure 3. The impact of the divergence of actual TDS slopes from the model TDS slopes in the old TDSTAB reference file used by the pipeline. The top row is for observations obtained during Cycle 26, and the bottom row for observations obtained over a year later during Cycle 27. The left panels show the fractional residuals of the calibrated fluxes against CALSPEC model spectra `gd71_mod_010.fits` against wavelength, and the right panels show the histogram of residuals. The residuals have been obtained over 5 Å bins, which are used for deriving the TDS slopes. In each case the dashed lines mark the nominal 2% tolerance limits.

introduced, the existing reference file slopes are identically zero, as shown by the dashed cyan line.

In the non-overlapping regions, only one or other of the cenwaves is used, and effectively there is no averaging. At several wavelengths in the overlap region between about 1625 and 1750 Å, the differences between the cenwave 1577 and cenwave 1623 slopes are significant - up to about 1% per year. Even by eye, it is possible to discern the detector position dependence, particularly towards the short wavelength end, where the values are about -3% per year in the 1578–1610 Å region for cenwave 1577, and in the 1625–1660 Å region for cenwave 1623.

The effect of using cenwave dependent slopes was explored by creating two

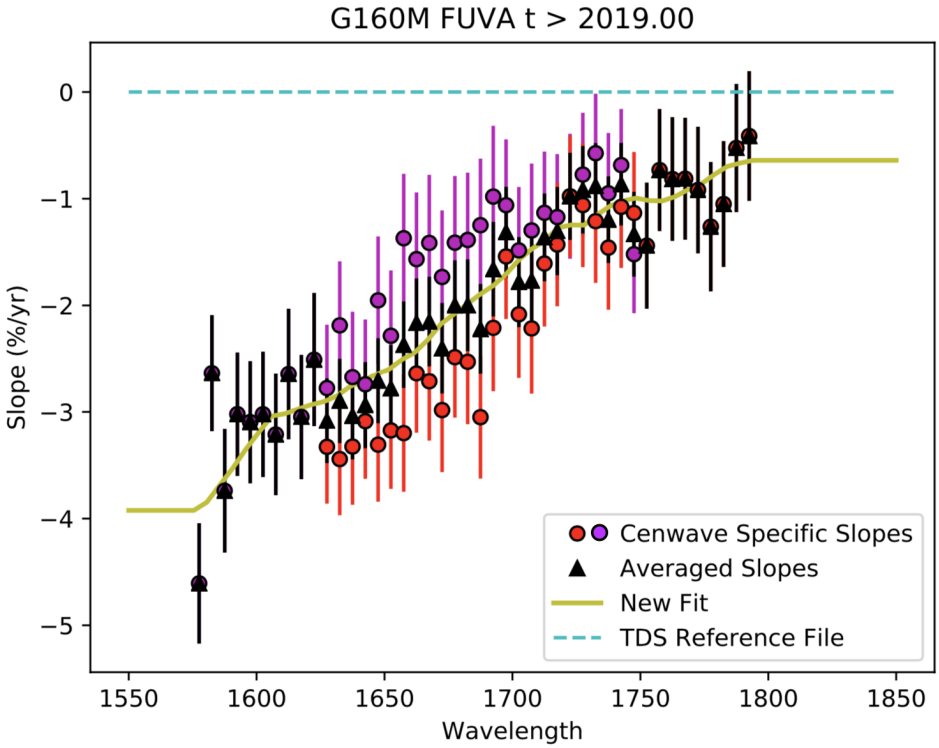

Figure 4. The TDS slopes measured for G160M/1577 (purple circles) and 1623 (red circles), their averages (black triangles), and the slope fit to these averages (yellow line). The dashed blue line is identically zero, since the current TDS reference file does not have a break point at 2019.0

TDSTAB reference files based on the same set of observations, one with slopes averaged in the usual way, and the other using cenwave dependent slopes for the monitored modes. The TDS parameters for these files were derived from all monitoring data up to visits 53 and 54 of the Cycle 27 program. The observations obtained during visits 05 and 06 were calibrated using each of these new TDSTAB reference files, and compared the output with the existing calibration. Fig. 5 shows the results for the GD71 observation using G160M/1577/FUVA obtained during visit 06. The plots in the left column show the flux residuals between the calibrated data and the GD71 CALSPEC model (`gd71_mod_010.fits`). In each case, the blue dots are the results using the old (then current) TDSTAB, and the red crosses are the results of the newly derived TDSTAB files. The dashed lines mark the nominal 2% in accuracy required. The right column panels show histograms of the residuals. Significant improvement in the calibration is evident in the region between about 1630 and 1700 Å where cenwaves 1577 and 1623 overlap. Towards the short wavelength edge, where there is no overlap between cenwaves 1577 and 1623, the two reference files yield nearly identical results, as expected.

After this analysis had been completed, the final standard mode TDS parameters

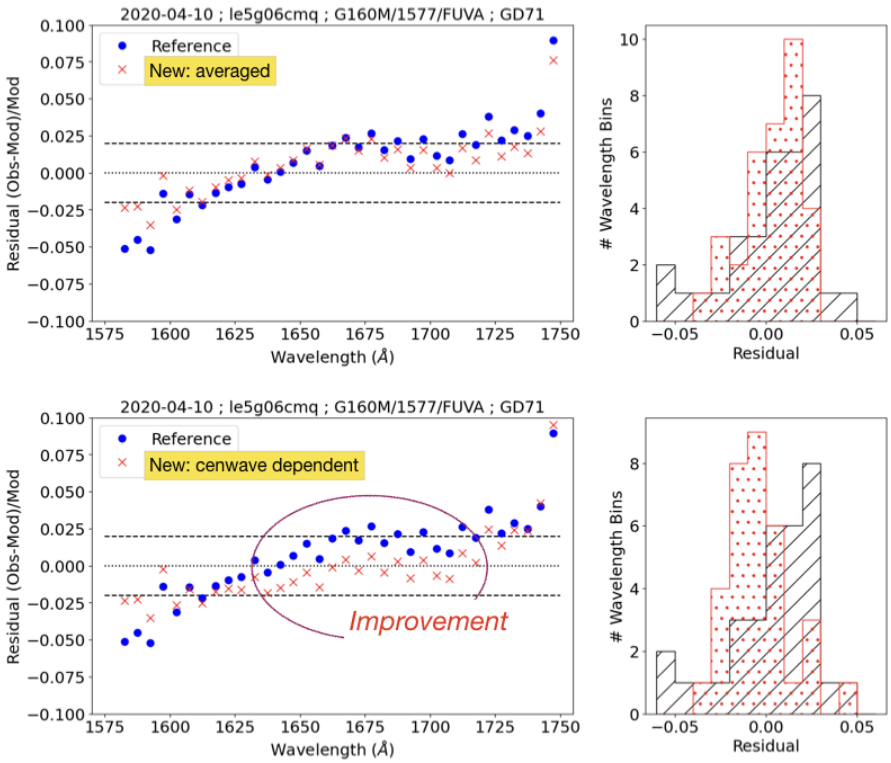

Figure 5. The fractional residuals (left column) and histograms (right column) comparing flux calibrations done with different TDSTAB files for a monitored mode G160M/1577/FUVA observation. The residuals are calculated relative to the CALSPEC model `gd71_mod_010.fits`. In both rows, the blue dots show the results using the previous TDSTAB used by the pipeline, and the red crosses show results using newly derived TDSTAB files. The wavelength region where the cenwave dependent slopes show a clear improvement is labeled in the bottom-row plot. Note that the cenwave dependent TDSTAB used in this analysis is an intermediate version and **not** the final delivered file.

were derived using cenwave dependent slopes and using all monitoring data up to, and including, visits 05 and 06 of the Cycle 27 program. The scientific testing was done using observations obtained during the later visits, 07, 57, 08, 58 and 09. (Visits 10 and 11 were executed after the delivery of the new reference files.) As part of the scientific testing, we verified that there were no changes in the results for the original LP4 Flux Calibration progam (PID: 14910, PI: Rafelski). These new cenwave dependent models allow us to reach our 2% accuracy flux calibration goal. After the scientific testing, the rows for G130M/1055, 1096 (the "blue-modes") and for G160M/1533 and G140L/800 (the "new cenwaves") were copied over to the newly created TDSTAB reference file

from the previous reference file, 46t1623fl_tds.fits.

TDSTAB files are not Lifetime Position (LP) dependent. The hybrid cenwave dependent parameters were tested only at LP4. Therefore the new file delivered has a USEAFTER date of October 2, 2017, when COS operations at LP4 started. The TDS slopes at LP4 and LP3 have been shown to be the same, based on an analysis of observations obtained during the Cycle 25 monitoring program (PID: 15384, PI: Sankrit), which have been described in Sankrit (2019). Therefore the new TDSTAB file will be valid for any specially commanded LP3 observations that have been obtained since the move to LP4, or that will be obtained in the future. Additionally new sensitivity curves for the standard modes were backed-out using the updated TDS parameters, and updated FLUXTAB reference files for LP4 and LP3 were created. The LP3 file has a USEAFTER date matching that of the new TDSTAB file.

5. Reference Files Delivered

Three reference files were delivered to CRDS for use in the CalCOS pipeline: the TDSTAB file, 4a52019el_tds.fits, and associated FLUXTAB files for use at LP4, 4a52019cl_phot.fits, and LP3, 4a52019fl_phot.fits. The TDSTAB and LP3 FLUXTAB reference files have USEAFTER dates of October 2, 2017, which was the start of COS operations at LP4. These files were activated in the CRDS on October 6, 2020.

6. Continuation Plan

In Cycle 28, the regular monitoring of the FUV TDS continued in program 16324 (PI: K. Rowlands). The targets and frequency of visits are the same as in Cycle 26. Additional observations at LP3 and LP5 are planned to support the flux calibration of modes that will move to these new lifetime positions.

Change History for COS ISR 2021-02

Version 1: 8 March 2021- Original Document

References

Bostroem, K. A., et al. 2015, COS Technical Instrument Reports 2014-05
De Rosa, G., Sana, H., Ely, J. and the COS team, 2016, COS Instrument Science Report 2016-13
De Rosa, G. and the COS team, 2017, COS Instrument Science Report 2017-10
De Rosa, G. and the COS team, 2018, COS Instrument Science Report 2018-09
Oliveira, C., et al. 2018, COS Instrument Science Report 2018-16
Osten, R. A., et al. 2010, COS Instrument Science Report 2010-15
Osten, R. A., et al. 2011, COS Instrument Science Report 2011-02

Sankrit, R. 2019, COS Instrument Science Report 2019-18
Sankrit, R. 2020, COS Instrument Science Report 2020-06